ISABE-2001-1194

Numerical Flow Simulation of a Counter-Rotating Fan Stage, using a RANS Solver for Unstructured Grids

A. I. Georgiadis, D. G. Koubogiannis, K. C. Giannakoglou and K. D. Papailiou,
Laboratory of Thermal Turbomachines,
National Technical University of Athens,
GREECE
e-mail: kgianna@central.ntua.gr

1 Abstract

A Navier-Stokes equations solver based on unstructured grids with triangular elements is used for the numerical simulation of the transonic flow through the fan stage of a counter-rotating propfan. Two rotors with 5/6 pitch ratio and a small axial gap between them are modelled at constant radius, using quasi-3D considerations. The flexibility that unstructured grids offer in discretizing complex domains is extended to multi-row computations, by generating time-varying grid zone(s) to span the inter-row gap(s). The lagged periodic boundary conditions on either blade row grids are treated through coordinate transformations, in accordance with the inclined computational plane theory. The Spalart-Allmaras one-equation turbulence model is used to effect closure. The two-rotor fan stage results are compared with measurements as well as other available numerical predictions.

2 Introduction

The relative motion of rotors with respect to upstream or downstream stators (or other counter-rotating rotors, as in the present study) is a major source of flow unsteadiness. Aiming at the improvement of single- and multi-stage compressors' performance, the relevant flow phenomena call for accurate modeling, especially in case of closely spaced rows. The advent of modern parallel- or super-computers enables the numerical modeling of the so-called Rotor-Stator-Interaction problem (this will be referred to as RSI even in case of two rotors), by developing CFD codes which are capable of performing multi-row computations.

Two are the key-problems associated with the development of Navier-Stokes solvers for RSI problems: (a) the accurate and easy enforcement of periodicity conditions in case of unequal pitches of non-integer ratio and (b) the accurate communication of flow quantities between adjacent rows. Over and above, computational cost and storage requirements should be kept as low as possible.

Concerning the enforcement of periodic conditions over the appropriate grid nodes, the mixing-plane technique proposed by Erdos [1] and used by a limited number of researchers suffers from large computer storage and the invalidity of its basic assumptions in viscous flows. The time-inclined computational plane approach introduced by Giles [2], [3] is a viable alternative to the problem at hand and, for this reason, it has found widespread use. A noticeable feature of this technique is its moderate computer storage requirements, given that results for the entire last period should be stored at the end, for post-processing reasons.

Different schemes for exchanging data across the interfaces of subsequent rows have been devised and published. They depend on the type of grids used to model the computational domain in each one of the rows. In the literature, the existing interfacing

schemes can be classified to patched, overlaid and those using auxiliary shearing grid zones. A common practice is to generate single- or multi-block structured grids on each row, which abut each other along the patch boundary. As they slip past each other, 1D (for 2D problems) or 2D (for 3D problems) interpolations at the interface are employed [4], [5], [6]. Conservative second-order interpolations are employed [4], though non-conservative schemes have also been used for low-Mach number flows [5]. For transonic turbines, Giles [3] used structured grids for each row, separated by a cell width at the interface. Working with equal grid node spacing along the interface on either side, a set of quadrilaterals were redifined at each new time-step, by applying the nearest neighbour connection rule. Our approach is the unstructured-grid variant of his method; as it will become clear as the paper develops, the use of unstructured grids with arbitrary grid node spacings along the interface and the replacement of quadrilaterals with triangles increases flexibility.

In the present paper, a vertex-centered, finite-volume RANS solver for compressible unsteady flows which uses unstructured grids with triangular elements [7], is modified in order to account for the RSI problem. A dual time-stepping technique is used, combined with a pointwise implicit Gauss-Seidel scheme to converge the linearized equations at each time-step. The method is second-order accurate in both time and space and uses the Spalart-Allmaras model to compute the eddy-viscosity coefficient.

A distinct computational domain is defined for each row, leaving small axial gaps between this and the downstream boundary of the upstream row or/and the upstream boundary of the downstream row. No restriction for the grid nodes distribution along these boundaries are imposed.The gap is filled by series of triangles formed between the surrounding nodes. At each time-step, the interfacial grid is regenerated. By doing so, each grid node and the corresponding integration cell belong to a single domain (i.e. row) and are treated accordingly.

The fan-stage of an ultra-high-pass propfan engine, investigated aerodynamically at DLR [8], [9], will be analyzed through the developed software. The stage consists of two counter-rotating rotors, with pitch ratio equal to 5/6. Results will be compared with measurements as well as other numerical predictions (by DLR, too).

3 The RANS Solver

The Favre-averaged compressible Navier-Stokes equations are discretized on an unstructured grid with triangular elements using a node-centered, finite-volume technique and solved through a dual time-stepping scheme. At each node, the control-volume is defined by successively connecting the midpoints of the edges incident upon the node with the center of the containment circle of each triangle, as proposed by Barth [10]. This is advantageous in case of grids stretched near the wall, where distorted cells with large aspect ratios exist.

For unsteady flow computations, the dual time-stepping technique is employed. Using the standard notation for 2D flows, the system of equations is written in vector form as

$$\frac{\partial \vec{U}}{\partial t} + \frac{\partial \vec{U}}{\partial \tau} + \frac{\partial \vec{F}}{\partial x} + \frac{\partial \vec{G}}{\partial y} = \vec{Q} \qquad (1)$$

where t stands for the real- and τ for the pseudo-time. $\vec{U}$ stands for the unknown vector $\vec{U} = h(\rho, \rho u, \rho v, E)$ and $h = h(x)$ is the streamtube thickness varying along the axial direction x. For the real-time derivative, a second-order trapezoidal scheme is employed. $\vec{Q}$ is the r.h.s vector with non-zero entries wherever $dh/dx \neq 0$. Equation (1) is discretized by separating real- (superscript n) and pseudo-time instants (superscript m) as follows

$$\frac{\vec{U}^{n+1,m+1} - \vec{U}^{n+1,m}}{\Delta\tau} + \frac{1}{2}\left(\frac{\partial \vec{F}}{\partial x} + \frac{\partial \vec{G}}{\partial y}\right)^{n+1,m+1} + \frac{\vec{U}^{n+1,m+1}}{\Delta t} = \vec{Q}^{n+1,m} + \frac{\vec{U}^{n}}{\Delta t} - \frac{1}{2}\left(\frac{\partial \vec{F}}{\partial x} + \frac{\partial \vec{G}}{\partial y}\right)^{n} \qquad (2)$$

For each real-time step, upon completion of the relative movement of the rows and the generation of the interfacial zonal grid (see below), pseudo-time iterations are carried out over each domain, separately, until the pseudo-time derivative vanishes. These iterations employ the Gauss-Seidel scheme. In our study, each period was decomposed in 100 real-time steps whereas about 150 pseudo-time iterations for each one of them was due. Information from the adjacent domain(s) is communicated, regularly.

The Roe approximate Riemann solver [11] is employed for the calculation of the inviscid fluxes, along with MUSCL-extrapolation for second-order accuracy. The required primitive variable gradients are computed using unweighted least-squares techniques, recommended for use in grids with high

aspect-ratio cells. The 2-D Barth-Jespersen limiter [10] was found absolutely necessary for stability purposes, otherwise the very stretched grid cells near the wall causes local overshootings and often breakdown of the code. The viscous terms are calculated by assuming linear distributions of flow quantities in each triangle. The Spalart-Allmaras turbulence model [12], written for compressible fluid flows [7] in the form of equation 1, is loosely coupled with the mean flow equations and solved using similar schemes. The implementation of the aforementioned turbulence model required source terms linearization, as a means to overcome numerical problems caused by their stiffness in the near wall region [12].

3.1 The Inclined Computational Plane Theory (IPT)

In order to account for periodicity in successive rows with unequal pitches, the inclined computational plane technique [2] has been adopted. This relies upon a transformation from the physical (x, y, t) to the computational (x', y', t') space, in order to obtain "spatial" periodicity by treating a single pitch area for each domain, minimizing thus memory requirements. For each row, the transformation reads $x' = x$, $y' = y$, $t' = t - \lambda y$, where $\lambda = \Delta T/P$ is the inclination parameter, ΔT is the difference of periods and P is the pitch of the actual domain. Through this transformation, equation 1 is written and solved in the form

$$\frac{\partial(\vec{U} - \lambda\vec{G})}{\partial t'} + \frac{\partial\vec{F}}{\partial x'} + \frac{\partial\vec{G}}{\partial y'} = \vec{Q} \qquad (3)$$

3.2 Treatment of the Interface

The successive rows are meshed separately. In order to facilitate the implementation of the turbulence model in the vicinity of walls, a number of pseudo-structured grid layers around each blade need to be generated first. The remaining domain is filled with a purely unstructured grid. The grid stretching ensures that the y^+ values of the first mesh points off the wall is below 1.

The outlet from the grid of one row and the inlet to the next row domain are usually defined at "one-cell" distance apart. At each time-step, the interdomain area is meshed anew, depending on the relative circumferential position of rows, whereas the two main computational grids remain intact. This intermediary mesh consists of a zone of triangular elements, with their nodes coinciding with the boundary nodes of the two basic grids. In the present study, it is just accidentally that the same number of nodes (26) have been distributed along the first rotor's outlet and the second rotor's inlet. In each time step, after employing the aforementioned transformation, the zone between two successive domains (which, after the transformation, are of equal pitch) is meshed. The zonal mesh is generated by linking nodes with edges according to some evident proximity rules. Details of the zonal grid can be seen in figure 1.

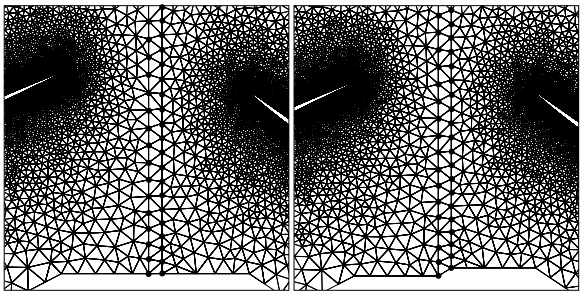

Figure 1: Details of the zonal grid generated between the two basic unstructured grids.

As previously explained, in the course of the pseudo-time integration, the two domains are treated separately. The zonal elements contribute to the formation of the computational cells at the adjacent boundary nodes of each domain. Thus, in the finite volume method, each interface node P is collecting contributions from its neighbours $K_N(P)$ belonging to the same domain as well as from neighbours lying in the adjacent domain, $Z_N(P)$, as in figure 2.

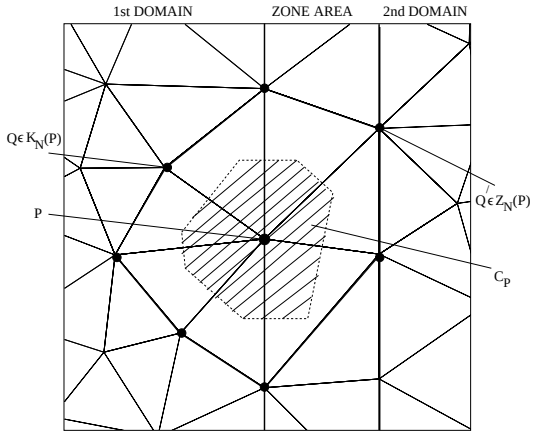

Figure 2: Finite-volume definition and dependencies for node P at the exit boundary of the first row.

3.3 Parallelization Aspects

Unsteady viscous computations, especially with multiple blade/airfoil rows in relative motion require excessive CPU time. Parallelization is a means to reduce the ellapsed computing time. Here, we employed a coarse-grain parallelization on a cluster of interconnected INTEL processors. The unstructured grid for each one of the rows was partitioned to as many subdomains as the number of available processors, with an equal number of grid elements each, and the minimum possible interface. To accomplish this, an in-house, genetic algorithm-based, partitioning tool [13] was used.

Practically, each row is treated in parallel whereas the inter-row area treatment follows in a sequential manner. The relative motion of the grids and the generation of the inter-row zonal grid are also sequentially carried out. However, it is beyond the scope of this paper to present parallelization aspects in full detail.

4 Numerical Results

4.1 The Counter Rotating Fan

The fan stage of a counter-rotating integrated shrouded propfan, investigated aerodynamically at DLR [8], [9], has been analyzed numerically through the proposed computational method. This case has been available from a research project entitled "Assessment of Physical Processes And Code Evaluation for Turbomachinery flows" (APPACET), funded by the European Union.

The fan stage consists of two counter-rotating rotors. The first of them consists of 10 blades (rotating counter-clockwise, at 4980 RPM) and the second of 12 blades (rotating clockwise, at 4316 RPM). The numerical simulation was quasi-3D, in the sense that it has been carried out over a cylindrical surface at radius R=0.353 m, by considering also the axial variation of streamtube thickness, as depicted in [8]. The computational domains for both rotors correspond to a single blade passage and the corresponding unstructured grids were generated according to the meshing guidelines mentioned elsewhere in this text. The two rotors' grids had 14107 and 12839 nodes, respectively. In Table 1, useful data for this case are provided. The linear velocity of each rotor is $U = 2\pi nR/60$ where n is its angular velocity. U_r stands for the relative velocity (absolute value) of each domain with reference to the adjacent one and period in each domain is given by $T = P_{(opposite\ domain)}/U_r$.

	Rotor I	*Rotor II*
P	$0.22179\,m$	$0.18483\,m$
n	$-4980\,rpm$	$4316\,rpm$
U	$-184.08\,m/sec$	$159.54\,m/sec$
U_r	$343.62\,m/sec$	
T	$0.000537\,sec$	$0.000645\,sec$

Table 1: Data (P = pitch, T = period)

The imposed boundary conditions correspond to the design operating point of the propfan. The inlet total pressure was 101325 Pa, the inlet total temperature 288.15K and the absolute inflow angle 0^o. The outlet static pressure was 98822 Pa. At the fan inlet, the boundary condition imposed to the Spalart-Allmaras equation was such that the turbulent viscosity was equal to 1% of the molecular viscocity.

4.2 Results and Discussion

In this section, numerical results obtained using the proposed method are compared with measurements and other computational data produced at DLR, during the APPACET project [14]. In figure captions, NUM (continuous lines) stands for the numerical results of the present method whereas EXP (marks) and OTH (dashed lines) stand for experimental and numerical data from DLR, respectively. Note that NUM and OTH have been obtained using similar discretization schemes and the same turbulence model, but on grids of different type (unstructured and structured, respectively).

Figure 3 illustrates computed isobar contours at six instants during the relative motion of the two rotors. In both rotors the flow is transonic and the shock generated in rotor-II interacts strongly with rotor-I. In this figure, $t = 0$ denotes the beginning of the first rotor's period (T1) after periodicity was established.

Figure 4 shows the pressure distribution over the rotor blade surfaces. Time-mean results for one period (rotor-I) are compared to numerical results from DLR. The time-averaged pressure recovery in rotor-I ("average" shock wave) is located downstream (about $0.06C_{ax}$) compared to the shock captured by the DLR method. Considering that both methods used the same turbulence model and the same flow data, differences could be attributed to the use of different grids (structured-unstructured) with different resolutions real the solid walls or/and to the effect of temporal parameters (time-steps, etc). On the other hand, the pressure distribution of rotor-II is in close agreement with OTH results

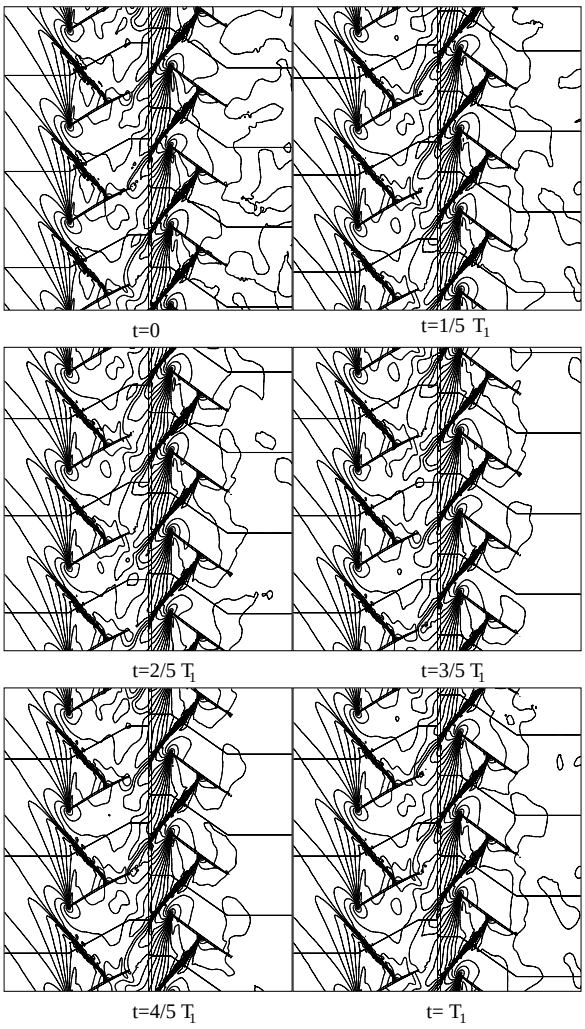

Figure 3: Isobar contours at six locations (0-5/5 T1, where T1 is the period of the first domain) of rotor-I with reference to rotor-II blades.

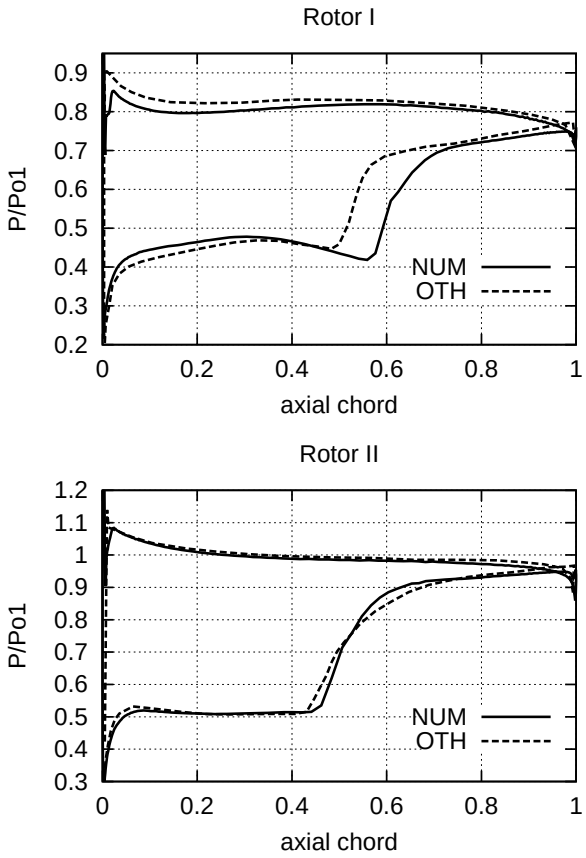

Figure 4: Blade surface pressure.

and the shock positions are almost identical.

Figures 6-9 illustrate relative velocity and flow angle distributions at four axial transversal stations, defined in figure 5. All distributions are time-averaged.

Each measuring station is associated with a single rotor; thus, stations M1 and M2 are linked to rotor-I whereas M3 and M4 with rotor-II and this is what "relative" stands for. It is interesting to note the close agreement between the two numerical predictions and even with measurements. Differences in the location of the upstream shock wave do not reflect on the upstream measuring station. Both predictions overestimate the velocity magnitude, a fact that should be attributed to small differencies in flow angles (i.e different velocity triangles; see figure 8) or even small differences in the (average) mass-flow rate (as determined by the inlet total pressure, the exit static pressure and the induced losses). In general, a satisfactory agreement was obtained for all stations but M4. Over the latter, the two numerical predictions behave similarly but deviate from measurements.

In figure 7 the so-called velocity amplitude (half the difference between maximum and minimum local velocity values, during a period time) distributions are shown. Good quantitative agreement with OTH and good qualitative agreement with EXP are observed.

Figure 8 shows relative angle distributions. Our predictions are in good agreement with experiments with the exception of the last measuring station, where differences of the order of two degrees can be seen. Finally, their fluctuation amplitudes are shown in figure 9. Differences can be found only in the rotor-II stations, where although NUM and OTH have almost identical average distributions, their fluctuation amplitudes show some slight differences (maximum 1 deg).

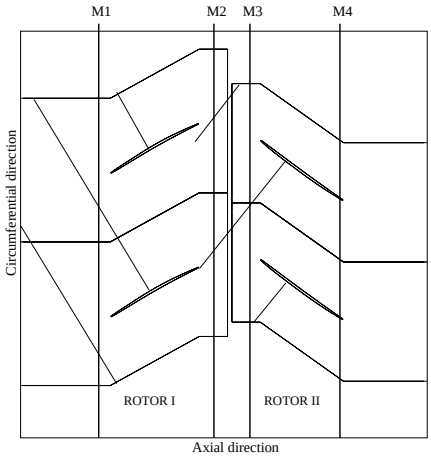

Figure 5: The four measuring stations locations (M1-M4) and the expected average shock-wave positions.

5 Conclusions

A method for the numerical simulation of multi-row 2D flow problems was presented. It is suitable for treating rows with unequal pitches, by meshing a single-blade passage per row with unstructured grids consisting of triangular elements. The proposed method exhibits great flexibility even in closely spaced rows due to the use of a separate unstructured zonal grid linking the upstream and downstream main computational grids. The use of unstructured grids for the entire flow domain alleviates restrictions inherent to other rival methods and yields low-storage requirements. The software parallelization, through the multiple-domain technique on a cluster of processors, significantly contributes to the reduction of computational cost. A counter-rotating fan of a propfan engine was analysed by means of a quasi-3D approach; the numerical predictions were in satisfactory agreement with measurements and other numerical predictions based on structured grids.

Acknowledgments

These authors would like to thank APPACET partners and especially DLR for making available measurements and computational results.

References

[1] Erdos J. I., Alzner E. and McNally W., 'Numerical Solution of Periodic Transonic Flow Through a Fan Stage', AIAA Journal, Vol. 15, pp. 1559-1568, 1977.

[2] Giles M. B., 'UNSFLO: A Numerical Method for Unsteady Inviscid Flow in Turbomachinery', Technical Report 195, MIT Gas Turbine Laboratory, 1988.

[3] Giles M. B., 'Stator/Rotor Interaction in a Transonic Turbine', AIAA Journal of Propulsion and Power, Vol. 6, pp. 621-627, 1990.

[4] Sbardella L. and Peiro J., 'Numerical Simulation of Rotor-Stator Inreraction in a Transonic Turbine Stage', CEAS International Forum on Aeroelasticity and Structural Dynamics, June 17-20, Rome, Italy, Vol. II, pp. 365-372, 1997.

[5] Rai M. and Madavan N., 'Multi-Airfoil Navier-Stokes Simulation of Turbine Rotor-Stator Interaction', ASME Journal of Turbomachinery, Vol. 112, pp. 377-384, July 1990.

[6] Rai M., 'Unsteady Tree-Dimensional Navier-Stokes Simulation of Turbine Rotor-Stator Interaction', AIAA Paper 87-2058, 1987.

[7] Koubogiannis D. G., Giannakoglou K. C., 'Implementation and Assessment of Low-Reynolds Turbulence Models for Airfoil Flows on Unstructured Grids', ECCOMAS 2000 Conference, Spain, 11-14 September 2000.

[8] Wallscheid L., Eulitz F., 'Investigation of Rotor/Rotor Interaction', ISABE 97-7186, 1997.

[9] Wallscheid L., Eulitz F., Heinecke R., 'Investigation of Unsteady Flow Phenomena in a Counter-rotating Ducted Propfan', ASME 98-GT-251, 1998.

[10] Barth T. J., 'Numerical Aspects of Computing Viscous High Reynolds Number Flows on Unstructured Meshes', AIAA Paper 91-0721, 1991.

[11] Roe P., 'Approximate Riemann Solvers, Parameter Vectors, and Difference Schemes', J. of Comp. Phys., 43, 357-371, 1981.

[12] Spalart P. and Allmaras S., 'A One-Equation Turbulence Model for Aerodynamic Flows', AIAA Paper 92-0439, 1991.

[13] Giotis A.P. and Giannakoglou K.C. 'An Unstructured Grid Partitioning Method Based on Genetic Algoritms', Advances in Engineering Software, Vol. 29, No.2, pp. 129-138, 1998.

[14] 'Assessment of Physical Processes and Code Evaluation for Turbomachinery Flows (APPACET)', European Union, Contract BRPR-CT97-0610.

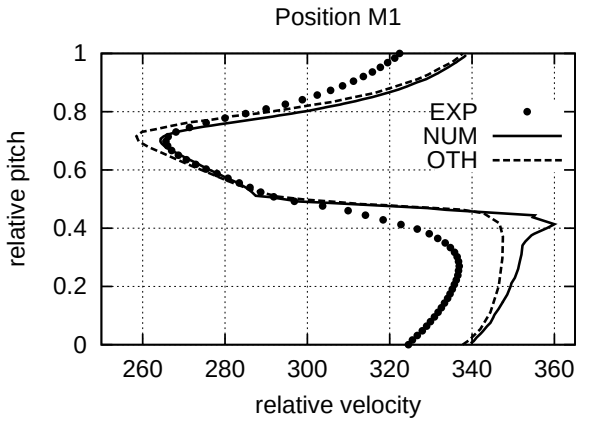

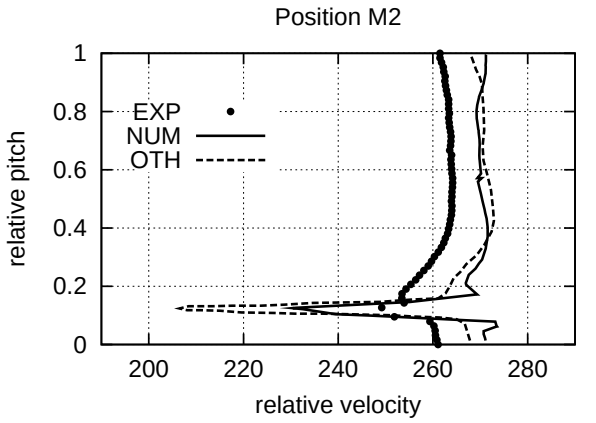

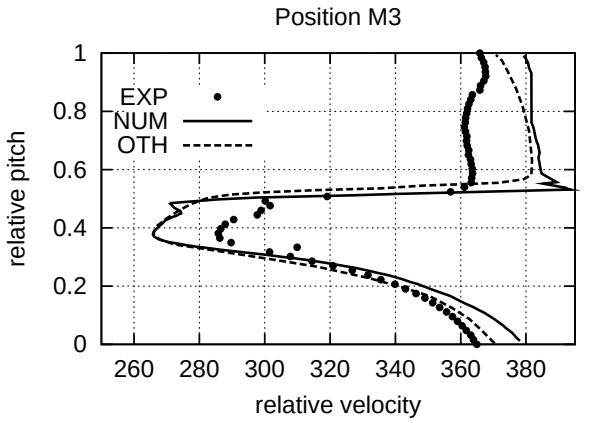

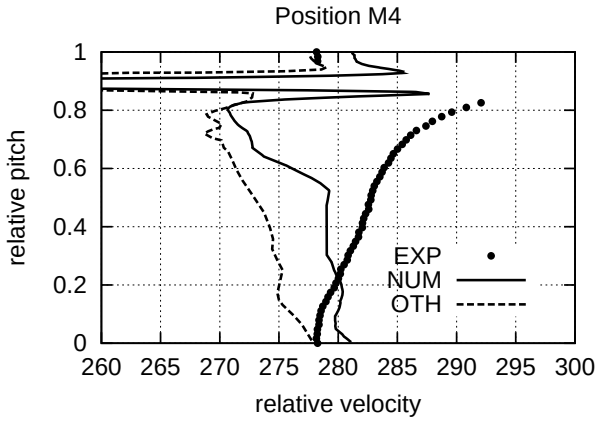

Figure 6: Relative velocity distribution at 4 axial positions.

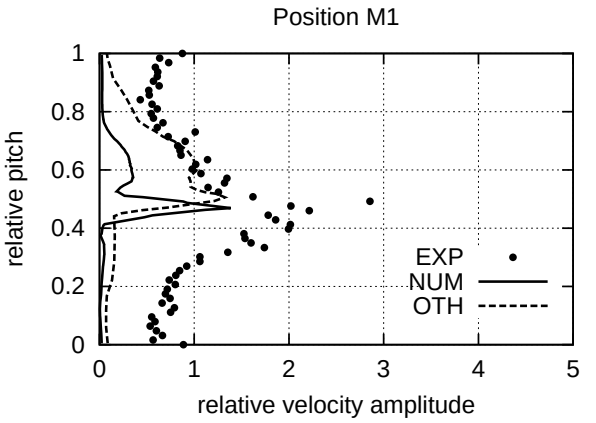

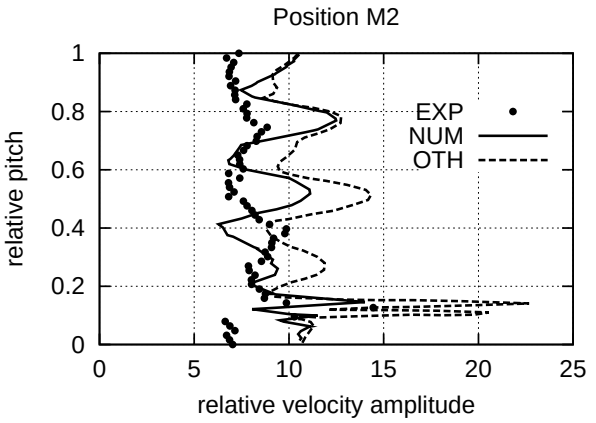

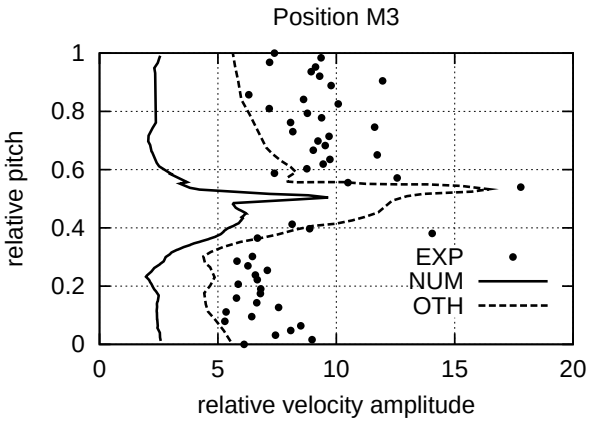

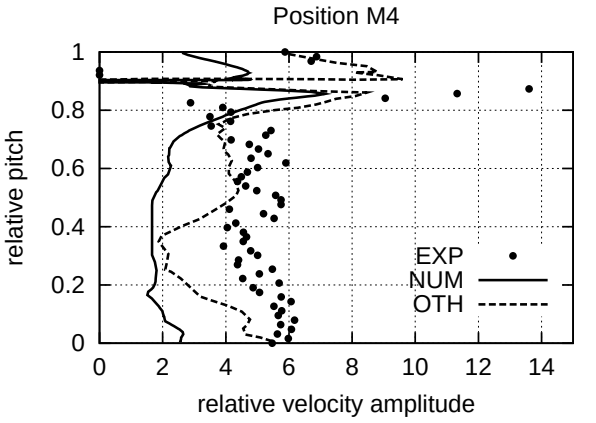

Figure 7: Fluctuation amplitude of relative velocity distribution at 4 axial positions.

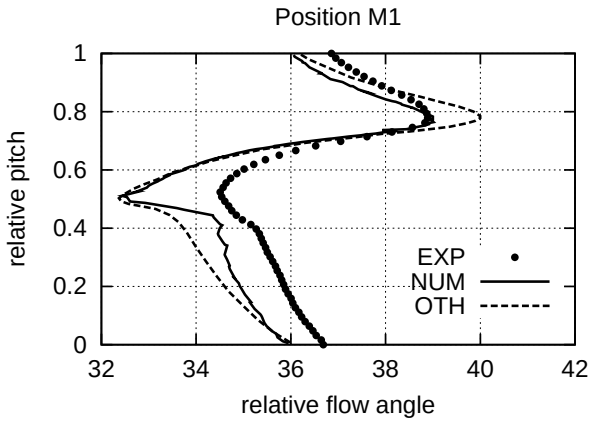

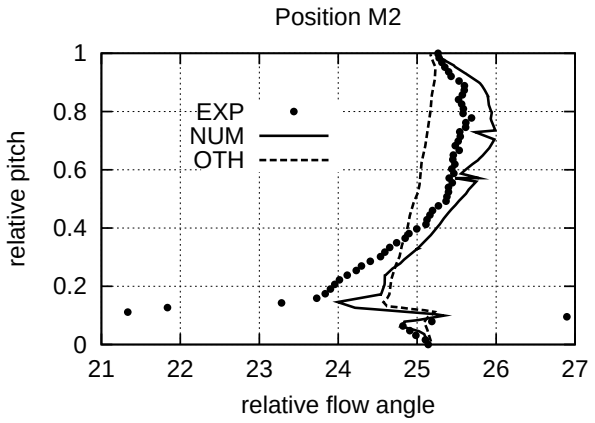

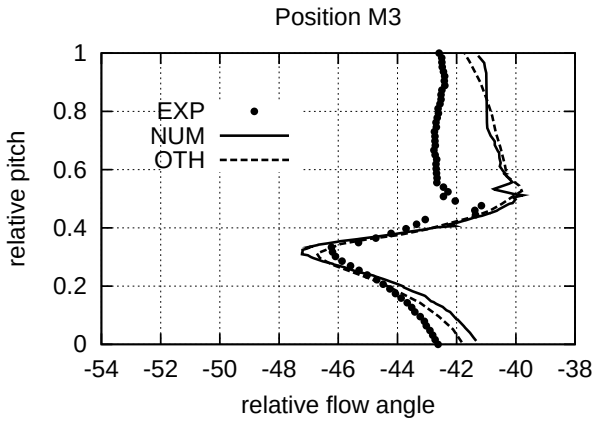

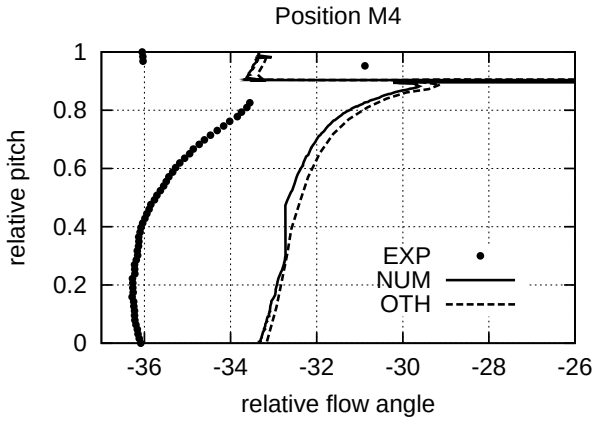

Figure 8: Relative flow angle distribution at 4 axial positions.

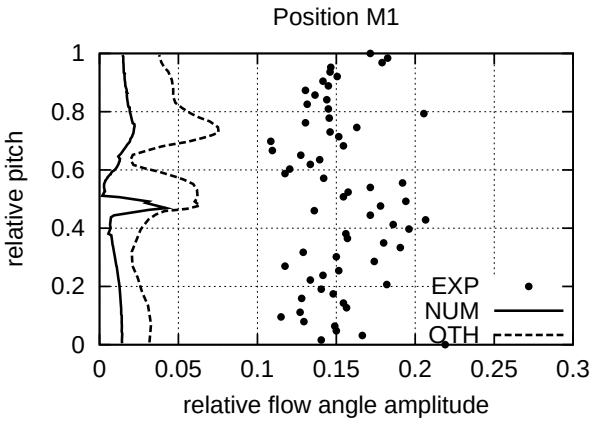

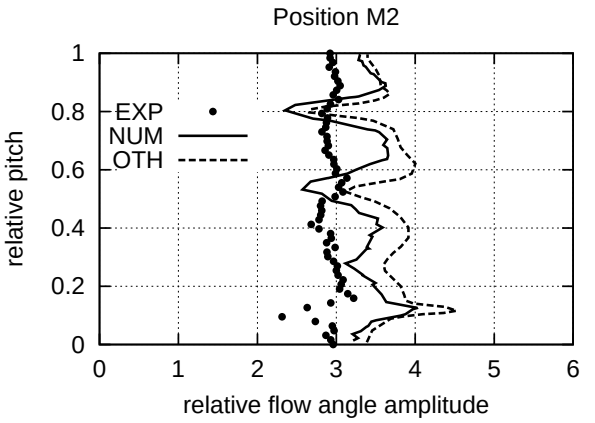

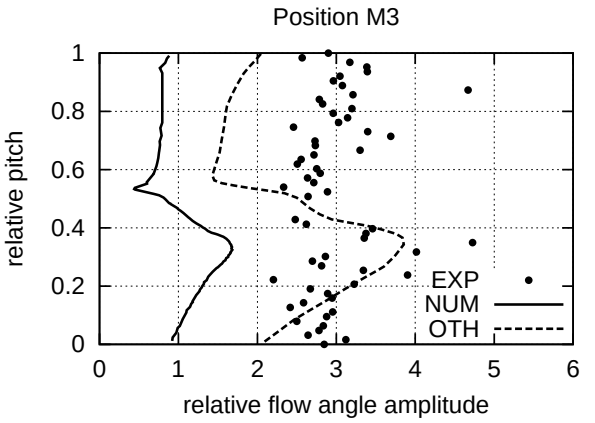

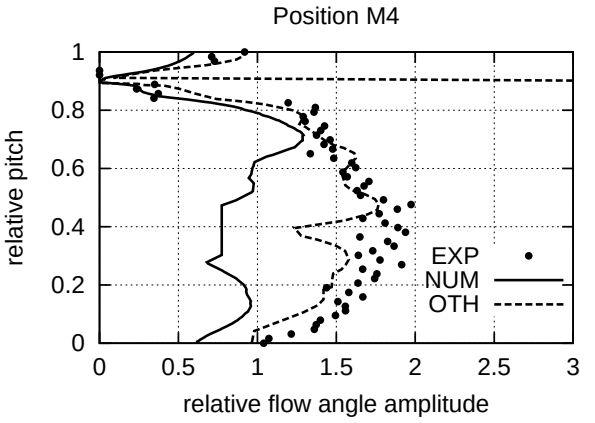

Figure 9: Fluctuation amplitude of relative flow angle distribution at 4 axial positions.